

Comparison of methods applied in photoinduced transient spectroscopy to determining the defect center parameters: The correlation procedure and the signal analysis based on inverse Laplace transformation

M. Suproniuk,¹ M. Pawłowski,¹ M. Wierzbowski,¹ E. Majda-Zdancewicz,¹ and Ma. Pawłowski²

¹Faculty of Electronics, Military University of Technology, Kaliskiego 2, 00-908 Warsaw, Poland

²Faculty of Physics, Warsaw University of Technology, Koszykowa 75, 00-662 Warsaw, Poland

(Received 11 September 2017; accepted 24 March 2018; published online 11 April 2018)

The procedure for determination of trap parameters by photo-induced transient spectroscopy is based on the Arrhenius plot that illustrates a thermal dependence of the emission rate. In this paper, we show that the Arrhenius plot obtained by the correlation method is shifted toward lower temperatures as compared to the one obtained with the inverse Laplace transformation. This shift is caused by the model adequacy error of the correlation method and introduces errors to a calculation procedure of defect center parameters. The effect is exemplified by comparing the results of the determination of trap parameters with both methods based on photocurrent transients for defect centers observed in tin-doped neutron-irradiated silicon crystals and in gallium arsenide grown with the Vertical Gradient Freeze method. *Published by AIP Publishing.* <https://doi.org/10.1063/1.5004098>

I. INTRODUCTION

The most commonly used method for research of defect centers in high-resistivity semiconductor materials is Photo-Induced Transient Spectroscopy (PITS).^{1–4} The method involves measuring a current flowing by a voltage-biased sample of semiconductor material as a result of illuminating it by a pulse of light, which causes filling the material's traps with charge carriers. Registered is a relaxation waveform of the photo-current caused by switching the light off. The photocurrent waveform is shaped mainly by a process of the thermal emission of the charge carriers from the traps and also by interactions of charge carriers with other traps located in the investigated material, as well as by generation and recombination processes. The photocurrent relaxation waveform associated with a single trap is an exponential decay, whose time constant is a reciprocal of an emission rate of charge carriers from the trap. Usually, at a given temperature, there are several traps that interact with charge carriers, so the photocurrent relaxation waveform is a sum of exponential functions. The energy model of a point defect is a defect center, which is described by an activation energy of the captured charge carriers and presented in a form of an energy level located in the band gap of the given semiconductor's energy band structure. The emission rate of charge carriers from a single defect center is dependent on the temperature and described by the Arrhenius equation,

$$e_T(T) = AT^2 \exp\left(-\frac{E_a}{k_B T}\right), \quad (1)$$

where E_a is the activation energy, parameter A is equal to a product of charge carriers' capture cross section σ and material constant γ , and k_B is the Boltzmann constant. Experimental determination of the dependence results in a set of pair-values (T , e_T) which allow identifying of the E_a and A parameters. When the pair-values are expressed as ($1000/T$, $\log(e_T)$), they describe a straight Arrhenius line. Then the activation energy E_a is estimated as a slope of the line and the parameter A

as the line's intercept. The values E_a and A unambiguously characterize the given defect center and, based on the existing knowledge base, are used to determine a microscopic structure of the defect.

To analyze the exponential photocurrent transients, there are two calculation procedures available: the correlation method^{4–6} and the advanced approximation procedure commonly called inverse Laplace transform.^{7,8} The procedures convert the recorded photocurrent relaxation waveforms to two-dimensional correlation and Laplace spectra, respectively. The spectra are presented in a coordinate system with axes being amplitude, emission rate, and temperature.⁹ In these spectra, thermal emission of charge carriers from defect centers is exposed in a form of a diagonal fringe which corresponds to a two-dimensional spectral peak. In order to determine the experimental temperature dependence of the emission rate of charge carriers, maxima of the fringe's sections are investigated. By projecting the maxima on a plane defined by the axes of temperature and emission rate, and by performing a linear regression of the maxima's positions, one obtains the line described by the Arrhenius equation (1).

In the case of the correlation spectrum, the fringe's sections are determined along the temperature axis, whereas in the case of spectrum obtained by the Laplace procedure, the sections are determined along the emission rate axis. It means that the ridge line of the fringe is defined by both methods differently.

A comparison of spectra obtained with both correlation and Laplace methods shows that the two procedures are complementary. However, the Laplace procedure is characterized by a higher resolution and therefore allows determining of parameters of a much larger number of defect centers than with the correlation method. On the other hand, the results obtained with this method are not always clear due to a high sensitivity of the procedure to noise which resides in the photocurrent relaxation waveforms. Hence, the low resolution correlation

spectrum, which gives a good image quality of the material's defect structure, can serve as a verification mean for spectra obtained with the inverse Laplace transform. In addition, the procedures can be supplemented and enhanced with advanced numerical methods that employ solutions to kinetics equations.^{10,11}

To illustrate the defect structure of a given material, the temperature dependences of emission rates of charge carriers from each of the detected defect centers, determined by the inverse Laplace transform, are laid on the spectral correlation surface projected on the plane defined by the axes of temperature and emission rate.¹² In many cases, incompatibility between the maxima of fringes' sections projected from both surfaces is observed. It causes that the defect center parameter values depend on the method used for the analysis of the photocurrent relaxation waveforms.¹³ The discrepancy makes it harder to correctly identify the defect structure of the material because the verification of measurement results is often performed by comparing the results obtained in other laboratories or stored in knowledge databases.

The fringes occurring on the experimental surfaces of correlation and Laplace spectra have various temperature dependences of the ridge lines' height. Their height may increase with temperature according to various slopes or show a bump-like maximum.¹⁴ The reason for this is diverse types of temperature dependences of the photocurrents' amplitudes. Since the calculations of the correlation procedure employ data obtained by directly sampling the recorded photocurrent waveforms, the nature of the temperature dependence of the amplitude has a direct impact on values of the experimentally determined parameters of the defect centers.

The aim of the study was to analyze and compare how the temperature dependence of the amplitude of the photocurrent relaxations impacts the course of the fringes' ridge lines occurring on the surface of the correlation spectrum and thereby also how it impacts the parameters of the defect centers being determined based on such a spectrum. It has been shown that the divergence between locations of spectral fringes obtained with both correlation and Laplace methods arises from a fitting mismatch of the model of photocurrent relaxation processes that is adopted in the procedure for determining the correlation spectral surfaces.

For this purpose, we conducted a purely simulation procedure of determining parameters of an exemplary defect center. We chose one of the authentic vacancy-oxygen-type defect centers observed in high-resistivity silicon irradiated with neutrons in a temperature range of 90–130 K. Parameters of the defect center were determined experimentally based on the Laplace spectrum.¹⁵ In the course of the simulation, we generated theoretical photocurrent relaxation waveforms for the assumed three different types of thermal dependence of their amplitudes, and then, based on the data, the correlation and Laplace spectral surfaces were produced. As a result, it was shown that parameters of the defect center determined based on both spectra are consistent only when the amplitudes of the photocurrent relaxation waveforms change according to the thermal dependence of the emission rate as described by the Arrhenius equation (1). By contrast, an inconsistency exists for most of the experimental results, meaning that the

parameters of defect centers measured so far with the correlation method are probably subject to substantial errors. It is assumed that spread of the measurement results of defect centers determined by various laboratories can reach $\pm 10\%$ for the activation energy E_a and an order of magnitude for the A coefficient.

Results of the analysis are then illustrated with images of the spectral surfaces, as well as by comparing parameters of detected defect centers for a sample of the FZ-grown (Float Zone) Si:Sn neutron-irradiated crystal in a temperature range of 35–130 K and for a sample of the VGF-grown (Vertical Gradient Freeze) GaAs crystal in a temperature range of 175–250 K. The spectral surface determined for the silicon sample shows that the amplitude of the spectral fringes increases with the temperature, while for the gallium arsenide one of the spectral fringes is characterized by a bump-like shape.

II. PROCEDURES FOR CREATING IMAGES OF THERMAL CHANGES OF TIME CONSTANTS OF PHOTOCURRENT RELAXATION WAVEFORMS

With the correlation method used to analyze defect centers, it is assumed that for each temperature T , a thermal emission of charge carriers from exactly one defect center is observed. Then the photocurrent relaxation waveform, acquired after switching off the illumination, can be described by an exponential expression,^{3,4}

$$i(t, T) = Q(T)e_T(T) \exp[-e_T(T)t], \quad (2)$$

where $Q(T) = n_{T0}(T)\mu(T)\tau(T)C(\lambda, T)qE$, n_{T0} is a concentration of the defect centers occupied by charge carriers at the moment of switching off the illumination, $\mu(T)\tau(T)$ is a product of lifetime and mobility of charge carriers, $C(\lambda, T)$ is a parameter that depends on a geometry of a region in which an occupation of the traps changes while the illumination is on, E is an electric field intensity, and q is the elementary charge.

The correlation method is computationally simple and consists in transforming the transient photocurrent waveforms $i(t, T)$ into a collection of K one-dimensional temperature spectra $S_{Ck}(T)$ obtained for each given value of the emission rate e_{Tk} , with $k = 1 \dots K$, according to the equation^{4,14,16,17}

$$S_{Ck}(T) = \frac{i(t_{1k}, T) - i(t_{2k}, T)}{i(0, T)}, \quad (3)$$

where t_{1k} and t_{2k} are the time moments at which the photocurrent waveform is sampled and $i(0, T)$ is the waveform's amplitude at the time of switching the illumination off. The values of the emission rate assumed for each of the K spectra are determined by time positions t_{1k} and t_{2k} of the samples of the photocurrent waveform. The time interval $[t_{1k}, t_{2k}]$ is called a window of emission rate for a value of e_{Tk} .^{3,12} A temperature T_{kmax} at which a maximum of the spectrum $S_{Ck}(T)$ occurs indicates that for this temperature, the time constant of the analyzed relaxation waveform is equal to a reciprocal of the emission rate e_{Tk} assumed for the determination of the Arrhenius relation,

$$e_T(T_{kmax}) = e_{Tk} = AT_{kmax}^2 \exp\left(-\frac{E_a}{k_B T_{kmax}}\right). \quad (4)$$

The dependence of the length of the emission rate window $[t_{1k}, t_{2k}]$ on its location is determined from a condition which specifies a position of the spectrum's maximum on the axis of temperature,^{12,14,16,17}

$$\frac{\partial S_{Ck}}{\partial T} = \frac{\partial S_{Ck}}{\partial e_T} \frac{\partial e_T}{\partial T} = 0. \quad (5)$$

And since the temperature dependence of the emission rate described by the Arrhenius equation (1) is a monotonically increasing function, the sufficient condition for (5) is that the derivative of the correlation spectra with respect to the emission rate, i.e., $\partial S_{Ck}/\partial e_T$, is equal to zero.

By considering Eq. (2) in Eq. (3), the correlation spectra can be formulated as a continuous function of temperature,

$$S_{Ck}(T) = F(T)e_T(T)\{\exp[-e_T(T)t_{1k}] - \exp[-e_T(T)t_{2k}]\}, \quad (6)$$

where $F(T)$ is a function dependent on the material-related parameter $Q(T)$ and the photocurrent's amplitude $i(0, T)$. It is assumed that the function $F(T)$ is constant with respect to the temperature, i.e.,

$$F(T) \approx F_0 = \text{const}, \quad (7)$$

as the temperature dependence of the function $F(T)$ is much weaker than the temperature dependence of the emission rate $e_T(T)$.^{12,14,16,17} Thus the condition $\partial S_{Ck}/\partial e_T = 0$ can be expressed as an equation,^{14,16}

$$\frac{1 - e_{Tk}t_{1k}}{1 - e_{Tk}t_{2k}} = \exp[-e_{Tk}(t_{2k} - t_{1k})]. \quad (8)$$

To obtain the relation between the emission rate and the time position of the photocurrent waveform's sample, Eq. (8) is numerically solved for assumed ratio $t_{2k}/t_{1k} = \alpha$. The most commonly assigned value is $\alpha = 3$, and thus the solution to Eq. (8) is^{12,14}

$$e_{Tk} = \frac{1.23}{t_{1k}} = \frac{3.69}{t_{2k}}. \quad (9)$$

As can be seen, the width of the emission rate e_{Tk} window depends on the time position t_{1k} of the starting sample of the window. For each pair of the time positions $(t_{1k}, 3t_{1k})$, a one-dimensional correlation spectra as a function of temperature are determined for an assumed set of K values of the emission rates e_{Tk} . The set of the one-dimensional spectra is transformed into a two-dimensional spectral surface $S_C(T, e_T)$, on which the thermal emission of charge carriers from defect centers appears as a fringe. Based on a ridge line of the fringe, which is described by the Arrhenius equation (1), determined are parameters of the observed types of defect centers.

Much better spatial resolution than with the correlation method may be obtained using an advanced approximation method called the inverse Laplace transformation.^{12,15} This method involves finding amplitudes of a set of exponential functions described by a given set of time constant values, which, when summed up, create the best-fit approximation of the photocurrent relaxation waveform. The waveform acquired for a temperature T_j , $j = 1 \dots J$ can then be expressed as the sum,

$$i(t, T_j) = \sum_{m=1}^M S_{Lj}(e_{Tm}, T_j) \exp(-e_{Tm}t), \quad (10)$$

where $S_{Lj}(e_{Tm})$ is the amplitude of the exponential function with a time constant which is a reciprocal of the emission rate, i.e., $1/e_{Tm}$, and M is the number of assumed values of the emission rates e_{Tm} ranging from $e_{T1} = e_{T\min}$ to $e_{TM} = e_{T\max}$.

The procedure of fitting the set of exponential functions to the photocurrent waveform $i(t, T_j)$ requires an inverse problem to be solved. As a result, the photocurrent waveform is transformed into a one-dimensional amplitude spectrum $S_{Lj}(e_T, T_j)$ as a function of the emission rate. On the spectrum, there are local extrema present, each one associated with the thermal emission of charge carriers from a corresponding type of defect center at the temperature T_j . The maxima are located along the emission rate axis. By analyzing changes in their position as a function of temperature, one derives the temperature dependence of the emission rate for the detected defect centers.

The procedures that implement the inverse Laplace transform are based on advanced methods of least squares and require a number of parameters that control the numerical process to be assumed. These parameters include, e.g., a number of emission rate points comprising the spectrum and minimum and maximum values of the emission rate range, i.e., $(M, e_{T\min}, e_{T\max})$. There are a number of algorithms developed and implemented as software programs like CONTIN,¹⁸ FTIKREG,¹⁹ NLREG,²⁰ and RILT.²¹ It should be noted that, in order to limit the number of solutions, the mathematical procedure for determining the spectrum $S_{Lj}(e_T, T_j)$ exploit the Tikhonov regularization. One of the most often used implementation is the CONTIN program, which was developed and made available for free by S. Provencher.²² It was designed to solve integral equations using Fredholm and Voltery equations of first kind. As in the case of the two-dimensional correlation spectrum $S_C(T, e_T)$, a two-dimensional Laplace spectrum $S_L(e_T, T)$ can also be calculated by arranging the one-dimensional spectra of the emission rate $S_{Lj}(e_T, T_j)$ obtained as a result of the analysis of the photocurrent relaxation waveforms acquired in a wide range of temperatures.^{12,15} The number of fringes occurring on the obtained surface indicates the number of defect centers interacting with charge carriers at the temperature T_j . Projections of the fringes' ridge lines on a plane defined by the axes of temperature and emission rate, similar to the correlation spectrum, can be described by the Arrhenius equation, which allows us to determine the parameters of the observed defect centers.

III. ASSESSMENT OF SUITABILITY OF CORRELATION AND LAPLACE SPECTRA

The assessment of suitability of both types of spectra for studying the defect structure of crystalline materials was performed by means of simulation. For this purpose, an exemplary defect center was assumed. We chose one of the authentic vacancy-oxygen-type defect centers observed in a temperature range of 90–130 K in a tin-doped neutron-irradiated high-resistivity silicon whose parameters are $E_a = 162$ meV and $A = 1.25 \times 10^7$ K⁻² s⁻¹, as determined experimentally based on the Laplace spectrum.¹⁵ The parameter values were assumed as the reference values. First, theoretical photocurrent relaxation waveforms for the given parameters were generated,

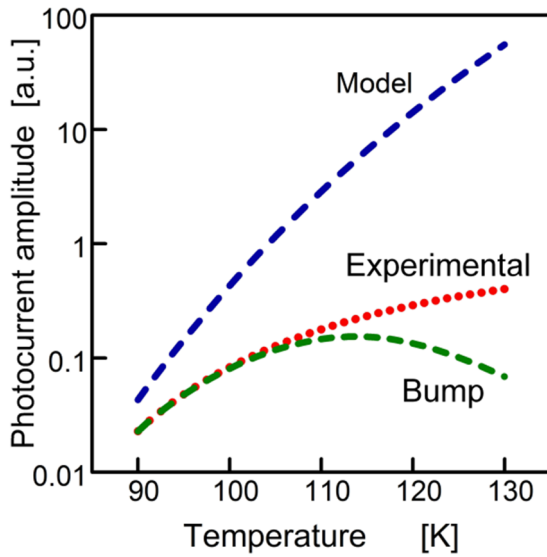


FIG. 1. Temperature amplitude dependences of simulated photocurrent relaxation waveforms assumed for simulation of the correlation and Laplace spectral fringes. The label “Model” denotes a dependence consistent with the theory, described by Eqs. (2) and (7). The label “Experimental” denotes a dependence observed for experimentally determined spectral fringes, whereas the label “Bump” denotes a dependence of the bump-like character.

and then the waveforms were transformed into the correlation and Laplace spectral surfaces. Finally, the parameters of defect centers obtained based on the location of the ridge lines of the spectral fringes were compared with the reference values. Observed differences allowed us to identify errors introduced by both procedures used for determination of the spectra.

To obtain the theoretical photocurrent relaxation waveform data, expression (2) was utilized. For a range of temperatures from 90 to 130 K at 1 K steps, the simulated waveforms were generated in a range of time from 0 to 43 ms at 1 μ s sampling period. Three different types of temperature dependences of photocurrent waveforms were assumed. The first one corresponded to a model described by Eqs. (2) and (7), which assumes that the photocurrent amplitude is dependent on the temperature only through the emission rate $e_T(T)$ described by the Arrhenius equation (1). We named this type of dependence a “model.” The second one is consistent with what is usually observed experimentally. It was defined based on an actual course of a spectral fringe’s ridge line’s amplitude determined for the V-O defect center.⁹ This type was named “experimental.” And the last one, although rarely occurring, also observed experimentally in some materials, e.g., GaN and SiC,^{14,24} resembles a bump or a hill, i.e., the temperature dependence has a maximum. Thus this type of the dependence was named a “bump.” All these three types of temperature changes or profiles of the photocurrent amplitude are shown in Fig. 1.²³

Spectral surfaces obtained with the correlation and approximation (i.e., Laplace) procedures based on the simulated photocurrent waveforms generated for the three assumed temperature profiles of the photocurrent amplitudes are shown in Fig. 2. It can be seen that the course of the fringes’ ridge lines correspond to the temperature dependences of the amplitude of the simulated relaxation waveforms. By comparing the spectra, some basic features of both methods emerge: the correlation method is characterized by a low resolution but a smooth spectral surface; on the contrary, the Laplace spectrum is characterized by a higher resolution but an irregular spectral

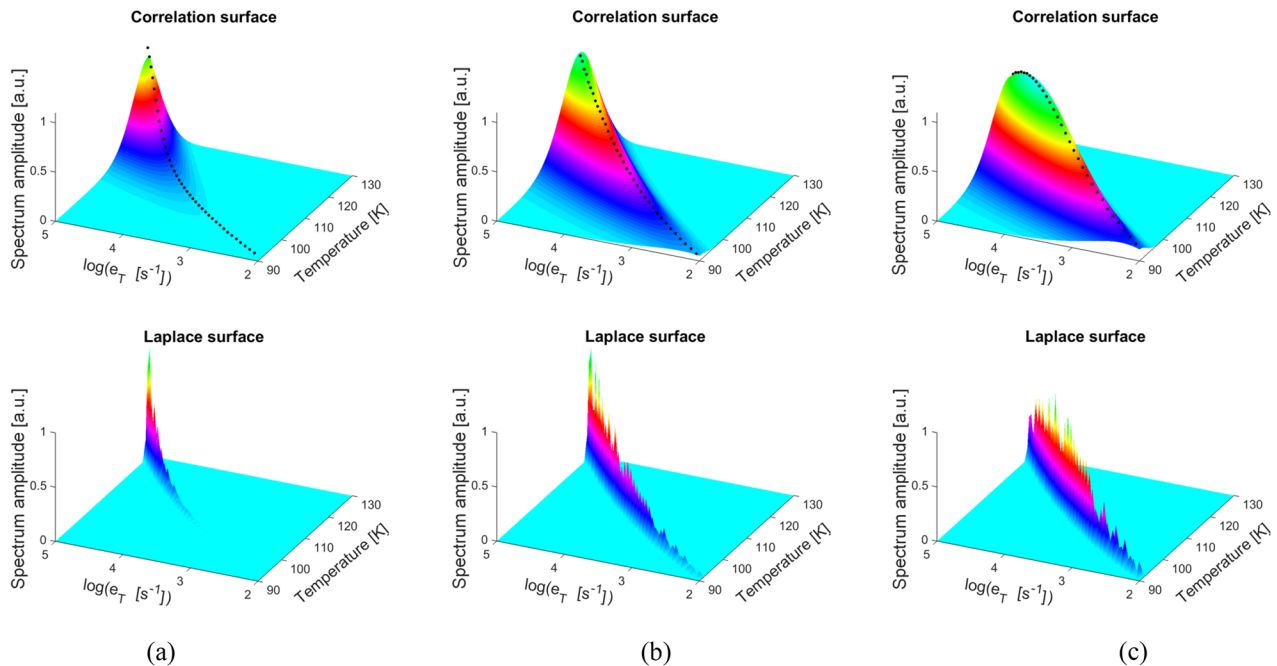


FIG. 2. Correlation (top) and Laplace (bottom) spectral fringes determined based on simulated photocurrent waveforms for three different temperature dependences of the waveforms’ amplitude as presented in Fig. 1: fringes corresponding to the profile labeled “Model” (a), fringes corresponding to the profile labeled “Experimental” (b), and fringes corresponding to profiles labeled “Bump” (c). Simulations were conducted for parameters of the V-O defect centers observed in the neutron-irradiated FZ Si:Sn in a range of temperature from 90 K to 130 K.

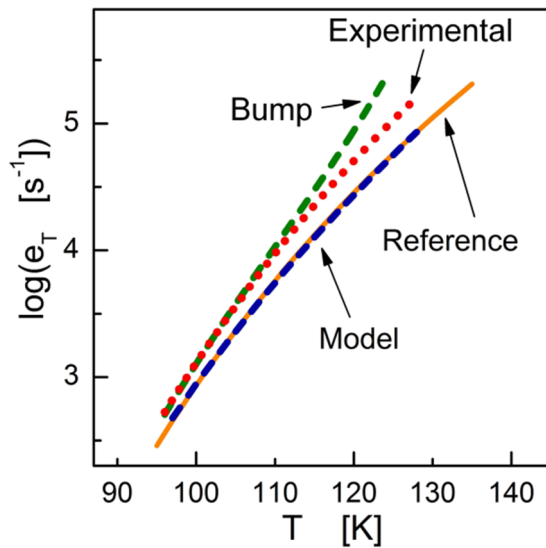


FIG. 3. Simulated temperature dependences of emission rate obtained by projecting the ridge lines of fringes seen on the correlation spectra in Fig. 2 on a plane defined by the axes of temperature and emission rate along with a reference line described by the Arrhenius equation (1) for parameters of the V-O defect center ($E_a = 162$ meV and $A = 1.25 \times 10^7$ K $^{-2}$ s $^{-1}$) assumed for the simulation of the investigated three types of temperature dependence of amplitudes of the photocurrent relaxation waveforms. The label “Model” denotes a dependence consistent with the theory, i.e., described by Eqs. (2) and (7). The label “Experimental” denotes a dependence observed for experimentally determined spectral fringes. The label “Bump” denotes a dependence of the bump-like character.

surface. The irregularity is caused by applying a discrete grid of temperature values and emission rate values. In case the relaxation waveform being analyzed for a given temperature is characterized by a time constant that does not correspond exactly to one of the values from the chosen emission rate grid, the CONTIN algorithm approximates the waveform using several exponential components. Besides, on the experimentally obtained Laplace spectra, an additional cause of the irregularities is present. It is the influence of a random component contained in the recorded photocurrent waveforms.

In order to show the influence of different temperature profiles of the photocurrent amplitude on the location of ridge lines on the spectral surfaces as well as on the parameters of defect centers, ridge lines of the spectral fringes from Fig. 2 were projected on a plane determined by the axes of temperature and emission rate (Arrhenius plot). Along with them, a reference line described by the Arrhenius equation (1) for the

reference parameters of the V-O defect center ($E_a = 162$ meV and $A = 1.25 \times 10^7$ K $^{-2}$ s $^{-1}$) assumed for the simulation was shown in Fig. 3. However, only ridge lines of the correlation spectra were shown in the plot, as the ridge lines of the Laplace fringes overlap completely with the reference line.

An evident deviation of the correlation spectral ridge lines labeled “Experimental” and “Bump” from the reference Arrhenius line can be seen. Only the ridge line labeled “Model” coincides exactly with the reference line. In this case, the temperature dependence of amplitudes of the simulated photocurrent waveforms satisfies the assumptions of the correlation method, what allows us to obtain correct values of the observed defect center parameters. Unfortunately, the actual temperature dependence of the amplitudes disagrees with the model assumptions. By approximating the lines with the Arrhenius equation (1), we obtained three sets of parameters of the simulated defect center in the form of activation energy E_a and factor A with the exception that for the “bump” profile, due to a visibly seen non-linearity and significant deviation of its ridge line from the reference line, the linear approximation was performed in two different ranges of temperature 95–110 K and 95–120 K labeled as “a” and “b,” respectively.

As the results in Table I show, correct evaluation of the parameters, regardless of the amplitude of the photocurrent waveforms, is assured only by the Laplace method, while the correlation method works only when the amplitudes change proportionally to the emission rate factor $e_T(T)$.²³ Moreover, as can be seen, the parameters associated with the “bump” profile for both temperature ranges differ. So, it is clearly seen that both the algorithm used and a temperature range considered for spectrum determination impact the accuracy of the parameter determination.

Obtained results were also shown in Fig. 4 on a plane defined by the axes of activation energy E_a and pre-exponential factor A . Parameters of the V-O defect center obtained based on experimental measurements were marked with blue Xs and labeled “V-O(C)” and “V-O(L)” depending on whether the parameters had been obtained with the correlation or the Laplace method, respectively. Parameters obtained based on simulated photocurrent waveforms were marked with red dots and labeled according to the photocurrent amplitude profile with labels defined in Table I. Also results of measurements of other defect centers observed in high-resistivity silicon were placed on the plot as black crosses and labeled according to their atomic configurations.^{25–27}

TABLE I. Summary of the simulation. Parameters and their 95% confident intervals for the V-O defect center observed in neutron-irradiated FZ Si:Sn, obtained from ridge lines of correlation and Laplace spectral fringes based on the simulated photocurrent waveforms for three profiles of the amplitude-temperature dependences. As the ridge line for the bump-like profile show a significant non-linearity, the defect center parameters in this case were evaluated separately in two temperature ranges. Note: For the simulation, the following V-O defect center parameters were assumed: $E_a = 162$ meV and $A = 1.25 \times 10^7$ K $^{-2}$ s $^{-1}$.

Photocurrent amplitude profile	Correlation method			Laplace procedure			Temperature range (K)
	E_a (meV)	A (K $^{-2}$ s $^{-1}$)	$A_{\min} - A_{\max}$ (K $^{-2}$ s $^{-1}$)	E_a (meV)	A (K $^{-2}$ s $^{-1}$)	$A_{\min} - A_{\max}$ (K $^{-2}$ s $^{-1}$)	
Model (M)	161 ± 3	1.21×10^7	$(1.30 - 9.74) \times 10^7$	162 ± 1	1.25×10^7	$(1.16 - 1.36) \times 10^7$	95–130
Experimental (E)	171 ± 3	5.19×10^7	$(4.31 - 6.06) \times 10^7$	163 ± 2	1.26×10^7	$(1.16 - 1.36) \times 10^7$	95–125
Bump (B _a)	177 ± 9	1.12×10^8	$(0.89 - 2.58) \times 10^8$	162 ± 5	1.25×10^7	$(1.01 - 1.74) \times 10^7$	95–110
Bump (B _b)	191 ± 7	5.60×10^8	$(4.10 - 8.83) \times 10^8$	162 ± 3	1.25×10^7	$(1.10 - 1.45) \times 10^7$	95–120

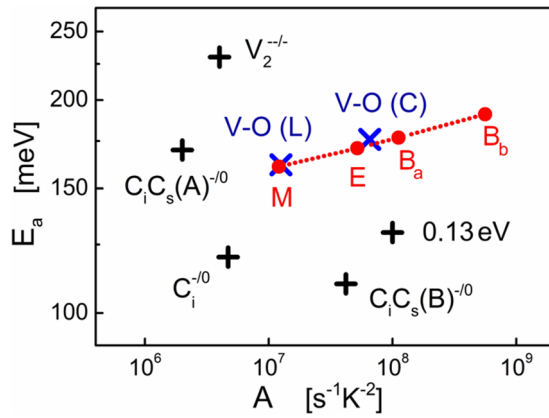


FIG. 4. Parameters of the V-O defect center observed in neutron-irradiated FZ Si:Sn obtained based on simulated (red dots) and experimentally measured (blue Xs) photocurrent waveforms, as given in Table I. The simulation-based parameters were marked according to the photocurrent amplitude profile with letters “M” for “Model,” “E” for “Experimental,” and “B_a” and “B_b” for “Bump” for two different temperature ranges. The dots show parameters obtained by the correlation method only, as the Laplace method gives same values regardless the amplitude profile. The measurement-based parameters marked with Xs were labeled according to the method used for their determination by “V-O (L)” for the Laplace one and “V-O (C)” for the correlation one. For a comparison, there were also parameters of other defect centers shown (black crosses), as observed in a high-resistivity silicon.^{25–27}

IV. EXPERIMENTAL RESULTS

Bearing in mind that the correlation method gives less accurate results, we decided to perform the same calculation as previously, based not on a simulation but on actual experimental data. Examples of Laplace and correlation spectral

surfaces for a tin-doped neutron-irradiated high-resistivity silicon crystal FZ Si:Sn are shown in Fig. 5. They were determined based on photocurrent relaxation waveforms measured in a temperature range of 35–130 K.^{9,15} For the determination of the Laplace spectral surface, the CONTIN program, developed by Provencher,^{18,22} was used. Solid lines show a projection of ridge lines of fringes occurring on the correlation spectral surface, while the broken lines represent the ridge lines from the Laplace spectral surface. Clear discrepancy between correlation and Laplace ridge lines can be seen on both surfaces. The ridge lines from the correlation surface are shifted toward lower temperatures compared to the ridge lines from the Laplace surface. These discrepancies result from the failure to meet the assumptions (7) by the amplitudes of the recorded photocurrent waveforms.

Parameters of the defect centers, obtained by approximating the ridge lines using the Arrhenius equation (1), were given in Table II. The results were also shown in Fig. 6 as points on a plane defined by the axes of activation energy E_a and pre-exponential factor A . Parameters determined using the Laplace method were marked with empty circles, whereas parameters determined using the correlation method were marked with solid circles. Parameters of other defect centers observed in the high-resistivity silicon^{25–27} were also placed on the plot as crosses along with their hypothetical atomic configurations.^{9,15} A significant difference in the parameter values determined with both methods can be noticed. The disparity complicates the process of comparison of the measurement results based on the defect center parameters obtained by various laboratories. Given the results of

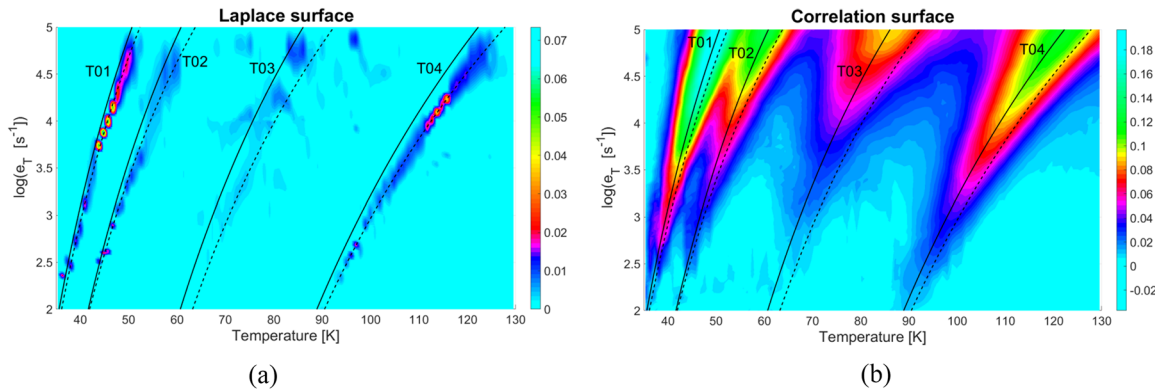


FIG. 5. Experimental Laplace (a) and correlation (b) spectrum surfaces determined for a neutron irradiated FZ Si:Sn crystal in a temperature range of 35–130 K. Lines show an approximation of projections of ridge lines of fringes occurring on the correlation (solid) and the Laplace (broken) spectral surfaces. Clear discrepancy between correlation and Laplace ridge lines can be seen.

TABLE II. Parameters of defect centers observed in neutron-irradiated FZ Si:Sn, determined experimentally using correlation and Laplace methods in a temperature range of 35–130 K. The confidence intervals of the parameters for 95% confidence level were given. Note: The labels (e) and (h) are used for electron and hole traps, respectively.

Defect center	Laplace procedure			Correlation method			Identification ^{9,15}
	E_a (meV)	A ($K^{-2} s^{-1}$)	$A_{\min} - A_{\max}$ ($K^{-2} s^{-1}$)	E_a (meV)	A ($s K^{-2} s^{-1}$)	$A_{\min} - A_{\max}$ ($K^{-2} s^{-1}$)	
T01	62 ± 10	3.41×10^7	$(1.2-11) \times 10^7$	64 ± 3	9.00×10^7	$(0.4-1.27) \times 10^8$	Sn-V ^{+/+} (h)
T02	64 ± 3	2.81×10^6	$(0.75-4.1) \times 10^7$	70 ± 5	1.70×10^7	$(0.5-2.38) \times 10^7$	C _i C _s (B) ^{0/+} (h)
T03	106 ± 15	7.06×10^6	$(0.25-1.38) \times 10^7$	110 ± 10	3.72×10^7	$(1.2-11) \times 10^7$	C _i C _s (A) ^{0/+} (h)
T04	162 ± 6	1.25×10^7	$(0.6-1.90) \times 10^7$	176 ± 7	6.55×10^7	$(1.9-12) \times 10^7$	V-O (e)

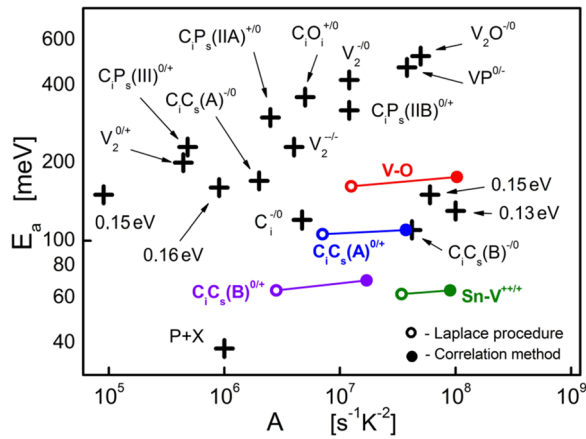


FIG. 6. Parameters of defect centers observed in a neutron irradiated FZ Si:Sn crystal measured in a temperature range of 35–130 K. Shown are parameters given in Table II obtained using the Laplace procedure (empty circles) and the correlation procedure (solid circles), as well as parameters of other defect centers (crosses) observed in a high-resistivity silicon.^{25–27}

analysis and simulation presented earlier, it can be assumed that the parameter values obtained using the Laplace method are more accurate than those obtained with the correlation method.

The correlation spectrum determined for the neutron-irradiated FZ Si:Sn crystal shown in Fig. 5 is characterized by an occurrence of single fringes whose ridge line's height increases as a function of temperature. However, often observed bump-shaped fringes are difficult to analyze as the disparity between ridge lines of fringes on the correlation and Laplace surfaces is larger.

An example of a spectral surface with the bump-like fringe on it is the correlation surface shown in Fig. 7 altogether with a corresponding Laplace spectrum. The spectra were determined based on experimental measurements of a Semi-Insulating (SI) GaAs crystal obtained with the VGF method in a temperature range of 175–250 K. The solid lines superimposed on both surfaces illustrate the fringes' ridge lines determined based on the Laplace spectrum and based on an approximation with the Arrhenius equation (1) and represent four defect centers detected in the material. Parameters of the defects, labeled T11–T14, were presented in Table III.

In this case, the resolution of the correlation method is not sufficient for the observation of a process of thermal emission of charge carriers from all defect centers in the given temperature range. Only the Laplace method allowed to easily observe the four defect centers. As can be also noticed, the fringe corresponding to trap T11 is clearly visible on the Laplace surface in a wide range of temperatures, i.e., from 180 to 230 K, whereas on the correlation surface the trap is visible only in a limited temperature range of 190–200 K as a bump-shaped fringe. In turn, the bump-like fringe observed in a temperature range of 200–230 K is a result of thermal emission of charge carriers from three traps, i.e., T12–T14. A complex character of the fringe is indicated by its asymmetrical shape, while the small resolution of the correlation method makes it difficult to estimate the number of traps associated with this fringe. On the other hand, the fringes associated with the T12–T14 traps, visible on the Laplace spectral surface shown in Fig. 7(a), are blurry and irregular, because of the sensitivity of the Laplace method to interference present in the photocurrent waveforms.

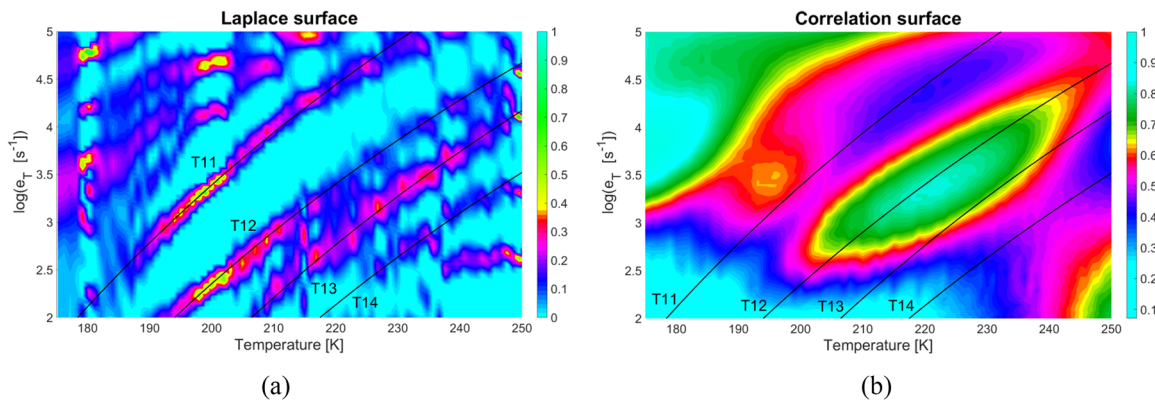


FIG. 7. Experimental Laplace (a) and correlation (b) spectrum surfaces determined for a VGF GaAs crystal in a temperature range of 175–250 K. Solid lines show an approximation of projections of ridge lines of fringes occurring on the Laplace spectral surface, representing four defect centers, labeled T11–T14, parameters of which were given in Table III.

TABLE III. Parameters of defect centers observed in a VGF SI GaAs crystal determined experimentally in a temperature range of 175–250 K based on the Laplace spectral surface. The confidence intervals of the parameters for 95% confidence level were given. Note: The labels (e) and (h) are used for electron and hole traps, respectively.

Defect center	E_a (meV)	A ($K^{-2} s^{-1}$)	$A_{\min} - A_{\max}$ ($K^{-2} s^{-1}$)	Identification ^{25,28,29}
T11	423 ± 7	2.8×10^9	$(1.6 - 5.6) \times 10^9$	Cu ^{-2/-} (h)
T12	421 ± 8	2.3×10^8	$(1.1 - 4.6) \times 10^8$	AsGa-VGa (e)
T13	471 ± 14	7.4×10^8	$(3.7 - 15) \times 10^8$	HB4 (h)
T14	464 ± 11	1.2×10^8	$(0.6 - 2.5) \times 10^8$	EB5 (e)

V. CONCLUSIONS

In the paper, for the first time presented was a comparison of correlation and inverse Laplace transform methods used for determining parameters of defect centers by the PITS analysis. It has been shown that the parameter values obtained with the correlation method may differ from the values obtained with the Laplace method. The reason for these discrepancies is a photocurrent relaxation model inadequacy adopted in the correlation method which assumes that the temperature dependence of the amplitude of the photocurrent relaxation waveform is only proportional to the temperature dependence of the emission rate. In practice, this assumption is usually not satisfied, what shifts the spectrum fringes associated with the thermal emission of charge carriers from defect centers on the spectral surface determined with the correlation method. And since the parameters of defect centers are determined by approximating the ridge lines of the spectral fringes with a line described by the Arrhenius equation (1), the obtained parameter values are subject to errors. The paper also shows a method based on inverse Laplace transformation, which allows us to obtain more precise parameters of defect centers regardless the nature of the temperature dependence of the photocurrent amplitude. Thus, the correlation method and the spectral surface obtained with it should mainly serve as a verification tool for the Laplace procedure as the spectral surface obtained with it may show irregularities in the spectral fringes caused by interferences in the experimental photocurrent waveforms. The conclusions may be helpful to people who study the defect structure of high-resistivity semiconductor materials, as well as other physical phenomena described by exponential functions, particularly on tasks involving solving ill-posed problems.

ACKNOWLEDGMENTS

The authors would like to express their thanks to Professor Pawel Kaminski and Dr. Roman Kozłowski from the Institute of Electronic Materials Technology in Warsaw for their helpful and valuable discussions at each stage of this work.

- ¹C. Hurtes, M. Boulou, A. Mitonneau, and D. Bois, *Appl. Phys. Lett.* **32**, 821 (1978).
- ²O. Yoshie and M. Kamihara, *Jpn. J. Appl. Phys., Part 1* **22**(4), 621 (1983).
- ³D. C. Look, *Semicond. Semimetals* **19**, 75 (1983).
- ⁴M. Brasil and P. Motisuke, *J. Appl. Phys.* **68**(7), 3370 (1990).
- ⁵D. V. Lang, *J. Appl. Phys.* **45**(7), 3023 (1974).
- ⁶G. L. Miller, J. V. Ramirez, and D. A. H. Robinson, *J. Appl. Phys.* **46**, 2638 (1975).
- ⁷L. Dobaczewski, P. Kaczor, I. D. Hawkins, and A. R. Peaker, *J. Appl. Phys.* **76**(1), 194 (1994).
- ⁸A. A. Istratov and O. F. Vyvenko, *Rev. Sci. Instrum.* **70**(2), 1233 (1999).
- ⁹M. Pawłowski, M. Miczuga, P. Kamiński, and R. Kozłowski, *Proc. SPIE* **4413**, 208 (2001).
- ¹⁰M. Suproniuk, P. Kamiński, R. Kozłowski, and M. Pawłowski, *Acta Phys. Pol., A* **125**(4), 1042 (2014).
- ¹¹M. Suproniuk, P. Kamiński, R. Kozłowski, M. Pawłowski, and M. Wierzbowski, *Opto-Electron. Rev.* **25**(3), 171 (2017).
- ¹²M. Pawłowski, P. Kamiński, R. Kozłowski, St. Jankowski, and M. Wierzbowski, "Metrology and measurement systems," *Pol. Acad. Sci., Comm. Meas. Sci. Instrum.* **12**(2), 207 (2005), available at <http://www.metrology.pg.gda.pl/no200502.html#p207>.
- ¹³P. Kamiński, R. Kozłowski, S. Strzelecka, A. Hruban, E. Jurkiewicz-Wegner, M. Piersa, M. Pawłowski, and M. Suproniuk, *Solid State Phenom.* **178-179**, 410 (2011).
- ¹⁴C. Longeaud, J. P. Kleider, P. Kaminski, R. Kozłowski, and M. Miczuga, *J. Phys.: Condens. Matter* **21**, 045801 (2009).
- ¹⁵M. Pawłowski, P. Kamiński, R. Kozłowski, and M. Miczuga, *Proc. SPIE* **5136**, 59 (2003).
- ¹⁶K. Yasutake, H. Kakiuchi, A. Takeuchi, K. Yoshii, and H. Kawabe, *J. Mater. Sci.: Mater. Electron.* **8**, 239 (1997).
- ¹⁷C. Longeaud, J. P. Kleider, P. Kaminski, R. Kozłowski, M. Pawłowski, and J. Cwirko, *Semicond. Sci. Technol.* **14**, 747 (1999).
- ¹⁸S. Provencher, Technical Report No. DA07, European Molecular Biology Laboratory, 1984.
- ¹⁹J. Weese, *Comput. Phys. Commun.* **69**, 99 (1992).
- ²⁰J. Weese, *Comput. Phys. Commun.* **77**, 429 (1993).
- ²¹I. G. Marino, MathWorks File Exchange Web Page: <https://www.mathworks.com/matlabcentral/fileexchange/6523-rlt>, 2007.
- ²²S. Provencher, Author's Web Page: <http://s-provencher.com/contin.shtml>, 2008.
- ²³M. Pawłowski and M. Suproniuk, *Electr. Rev.* **87**(10), 230 (2011), available at <http://pe.org.pl/abstract.pl.php?nid=5235>.
- ²⁴P. Kamiński, R. Kozłowski, M. Kozubal, J. Żelazko, M. Miczuga, and M. Pawłowski, *Semiconductors* **41**(4), 414 (2007).
- ²⁵R. Kozłowski, Ph.D. thesis (in polish), Institute of Electronic Materials Technology, Warsaw, Poland, 2001.
- ²⁶P. Kaminski, R. Kozłowski, and E. Nossarzewska-Orłowska, *Nucl. Instrum. Methods Phys. Res., Sect. B* **186**, 152 (2002).
- ²⁷P. Kaminski, R. Kozłowski, A. Jelenski, T. Mchedlidze, and M. Suezawa, *Jpn. J. Appl. Phys., Part 1* **42**, 5415 (2003).
- ²⁸P. Kamiński and R. Kozłowski, *Mater. Sci. Eng.: B* **91-92**, 398 (2002).
- ²⁹C. Bourgoin, H. J. von Bardeleben, and D. Stiévenard, *J. Appl. Phys.* **64**, R65 (1988).